Wide-Angle Pair Production and Quantum Electrodynamics at Small Distances*

J. D. BJORKEN,† S. D. DRELL, AND S. C. FRAUTSCHI†‡
Department of Physics, Stanford University, Stanford, California
(Received July 7, 1958)

Wide-angle photoproduction of high-energy electron-positron pairs in hydrogen is proposed and analyzed as a test of quantum electrodynamics at distances $\lesssim 10^{-13}$ cm. The effect of proton structure can be removed in terms of the two form factors measured in the elastic electron-proton scattering process. Cross sections are presented for two classes of pair production experiments: (1) those detecting one of the final particles, and (2) coincidence experiments. In addition to kinematic, anomalous moment, and nucleon form-factor corrections to the Bethe-Heitler formula, dynamical corrections to the proton current and radiative corrections are calculated. The final theoretical formula is believed to be accurate to 2%. A simple cutoff model suggests that a 5% accuracy in an experiment of type (1) tests the electron propagator at distances $\sim 0.7\times 10^{-13}$ cm, while a 10% accuracy in a coincidence arrangement of type (2) probes the electron propagator at $\sim 0.3\times 10^{-13}$ cm.

I. INTRODUCTION

WIDE-ANGLE photoproduction of high-energy electron-positron pairs in hydrogen probes the small-distance behavior of quantum electrodynamics. In particular, it offers the possibility of exploring the electron propagator at smaller distances than achieved so far.[1] This is possible because the effect of proton structure on the pair production matrix elements corresponding to the Feynman graphs of Figs. 1(a) and 1(b) can be completely and unambiguously summarized in terms of the two invariant form factors measured in the elastic electron-proton scattering process. With ambiguities which arise from interactions of nonelectromagnetic origin thus removed, the process in Fig. 1 yields new information on quantum electrodynamics at small distances if the virtual intermediate electron-positron line is far off the mass shell, as is the case for a high-energy interaction with large transfer of momentum.

In this paper we propose and analyze wide-angle pair production as an experiment which can increase our knowledge of the electron propagator in quantum electrodynamics by an order of magnitude.[2] We implement this proposal with a detailed, accurate calculation of the cross section which includes, in addition to kinematic and nucleon form-factor corrections to the Bethe-Heitler formula[3] contained in Fig. 1, dynamical corrections due to the proton current (Fig. 2), and radiative corrections (Figs. 3–4). The role of the proton in Fig. 2 corresponds to virtual Compton scattering and cannot be completely summarized in terms of the form factors of Fig. 1. The magnitude of these virtual Compton terms is the theoretical limiting factor of wide-angle pair production as a probe of quantum electrodynamics at small distances. The accuracy to which the pair production cross section can be measured and to which the proton form factors can be determined are the experimental limiting factors. They are indeed very severe ones since electrodynamic processes with large four-momentum transfer, needed to define a small distance, generally have exceedingly small cross sections.

We consider here two classes of pair production experiments: first, the type in which only one of the final particles is detected, and second, coincidence experiments. The detected particle in an arrangement of the first type must emerge with high energy at large angle with the incident photon direction in order to probe quantum electrodynamics at small distances. The most favorable condition for an experiment of this type appears to be to observe positrons at 90° with respect to an

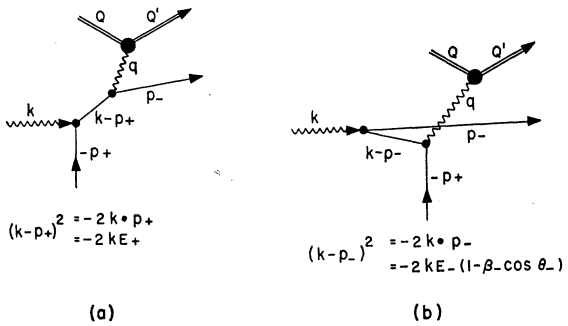

FIG. 1. "Bethe-Heitler" diagrams for pair production.

* This research was supported in part by the United States Air Force through the Air Force Office of Scientific Research. A preliminary account was presented at the Stanford Meeting of the American Physical Society, December, 1957 [Bjorken, Drell, and Frautschi, Bull. Am. Phys. Soc. Ser. II, 2, 392 (1957)].

† Holder of National Science Foundation Predoctoral Fellowship.

‡ Part of a thesis (by S.C.F.) submitted in 1958 in partial fulfillment of the requirements of a Ph.D. degree to the Department of Physics, Stanford University, California. Further calculational details will be found in this thesis.

[1] S. D. Drell, Ann. Phys. 4, 1, 75 (1958). In 1954, R. P. Feynman remarked upon the desirability and possibility of probing quantum electrodynamics at small distances by large-momentum-transfer experiments, such as wide-angle pair production. [R. P. Feynman, Anais acad. brasil. cienc. 26, 51 (1954)]. More recently, Budini, Poiani, and Reina [Proceedings of the Padua-Venice Conference on Mesons and Recently Discovered Particles, 1957 (to be published)] have observed that the nuclear form factors determined by electron scattering can be factored out of the Bethe-Heitler formula for bremsstrahlung in first Born approximation. They treat the nucleus as a fixed Coulomb source of charge Ze.

[2] All theoretical remarks made in this paper would apply equally well to bremsstrahlung, where γ rays are observed at large angles.

[3] H. A. Bethe and W. Heitler, Proc. Roy. Soc. (London) **A146**, 83 (1934).

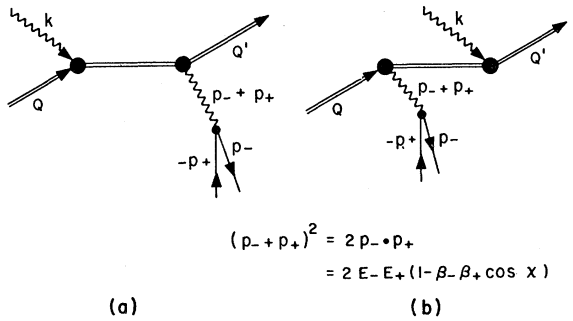

FIG. 2. "Compton" diagrams for pair production.

incident bremsstrahlung beam of peak energy 140 Mev. The limitation to this energy is dictated by the necessity of avoiding background from π^0 decays.[4] Also, at higher energies the resonance in the proton Compton effect[5] begins to introduce appreciable uncertainties into the analysis of the virtual Compton matrix elements of Fig. 2.

The distance to which quantum electrodynamics is probed in such an experiment is best seen from the Feynman diagrams in Fig. 1. In 1(a) the positron is produced directly at large angle with the incident beam and the intermediate electron line is $\sim$140 Mev off the mass shell for a positron energy of $\sim$100 Mev. This graph is sensitive to small-distance modifications of the propagator. On the other hand, in 1(b) the intermediate positron is nearly "real" and hence insensitive to small distance modifications. It is easy to see that the contribution of graph 1(b) is larger than that for 1(a) by a retardation factor $(1-\beta\cos\theta)^{-1}$, which when integrated over electron angles yields a factor $\ln(E_-/m)\sim 5$. Since only 20% of the cross section is sensitive to small-distance modifications, both an accurate calculation and an accurate experiment are required. A simple cutoff model suggests that a 5% accuracy is required to test the propagator at 0.7×10^{-13} cm.

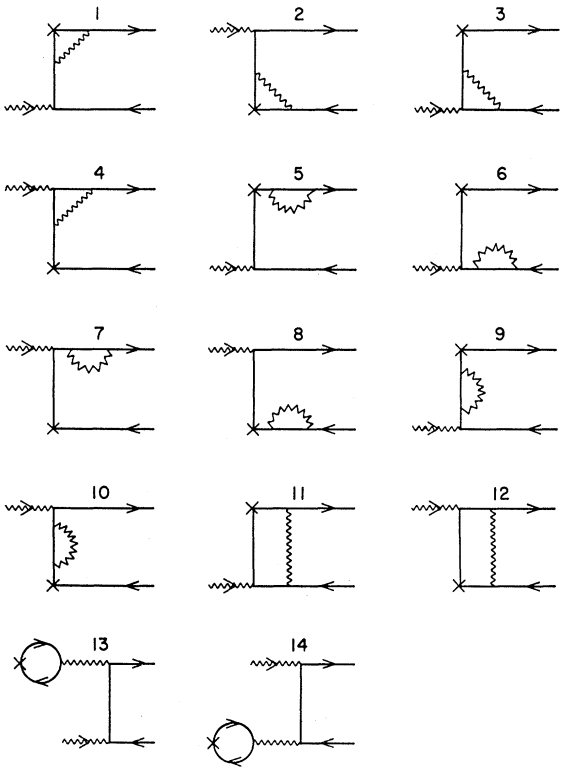

FIG. 3. Feynman diagrams for virtual radiative corrections.

To achieve this accuracy in the theoretical formula, we have recalculated the Bethe-Heitler formula integrated over electron angles with the following corrections included:

1. Kinematical corrections due to proton recoil in graphs 1(a) and 1(b) are kept through order q^3/M^3 $\sim$0.5%.

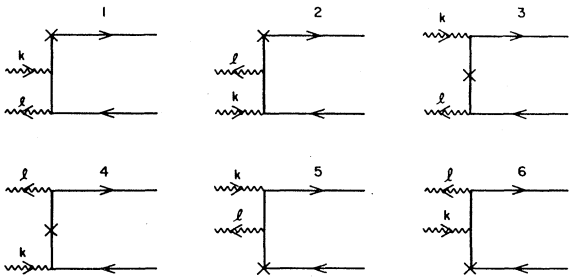

FIG. 4. Feynman diagrams for real photon radiative corrections.

2. The complete proton vertex is used in graphs (1) with the charge and moment form factors as measured by Bumiller, Chambers, and Hofstadter.[6] In performing integrations over final electron angles we have expanded these form factors as polynomials in q^2, retaining terms proportional to q^4, the limiting factor in the accuracy of this treatment being the present experimental uncertainty in the proton's charge distribution. For the choice of parameters discussed above, the static moment of the proton increases the theoretical cross section by roughly 10% above the Bethe-Heitler result, and recoil and finite-size corrections reduce it by a closely comparable amount. The present uncertainty in the proton's charge form factor leads to an uncertainty of less than 2% in the result.

3. Dynamical corrections due to the proton current as operating in Fig. 2 are calculated for a Dirac proton with observed anomalous moment. A point proton model is sufficient for the estimate of the importance of these terms since the role of the proton corresponds to virtual Compton scattering, which at 140 Mev is close

[4] We have in mind here experimental problems peculiar to the Stanford Linear Accelerator. We wish to thank Dr. W. K. H. Panofsky and Dr. B. Richter for informing us of these limitations.

[5] Yamagata, Auerbach, Bernardini, Filosofo, Hanson, and Odian, Bull. Am. Phys. Soc. Ser. II, 1, 350 (1956).

[6] F. Bumiller and R. Hofstadter, Bull. Am. Phys. Soc. Ser. II, 2, 390 (1957).

to its low-energy Thomson limit. This will not be so at energies near the pion-nucleon resonance. In the present analysis the contributions of the square of these terms and the interference terms with Fig. 1 are each less than 1% of the leading contributions from Fig. 1. This is due in part to two factors:

(a) The amplitude of the matrix elements in Fig. 2 is less than the Bethe-Heitler amplitudes of Fig. 1 by a factor $q/M\sim 0.2$.

(b) Because of retardation factors, the electron in Fig. 2 is preferentially emitted along the direction of the emitted positron, at 90° with respect to the forward direction, while in Fig. 1(b) the electron is preferentially emitted forward. This competition of angular factors reduces the interference terms between Fig. 1 and Fig. 2 by a factor $\ln(E/m)\sim 5$.

4. Radiative corrections to the leading-order matrix elements in Figs. 3–4 are calculated. Terms of order $\alpha\ln(E/m)$ relative to unity are retained and shown to alter the cross section by less than 1% for conditions in the present experimental arrangement.

Turning to the coincidence experiment, an arrangement which detects both the electron and the positron at large angles with respect to the forward direction has the important new advantage of making both Feynman diagrams in Fig. 1 sensitive to small-distance modifications of quantum electrodynamics. A symmetrical arrangement as in Fig. 5 with both electron and positron in the plane of the incident bremsstrahlung beam and at equal energies and angles (left and right) with respect to the photon direction has several extremely desirable features:

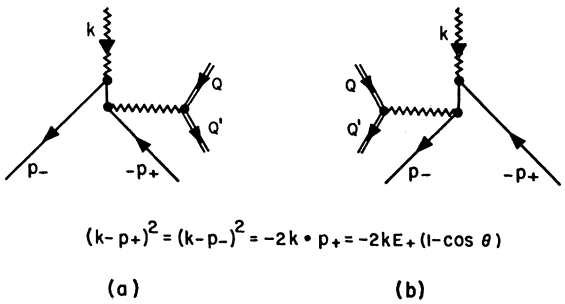

FIG. 5. "Bethe-Heitler" diagrams for coincidence experiment.

(1) An elementary charge conjugation argument shows that the interference term between the diagrams of Figs. 1 and 2 vanishes for such an arrangement.

(2) The square of the Compton diagrams (Fig. 2) can be made negligible by arranging the kinematics such that the proton recoil velocity is very small. Thus for a 550-Mev maximum energy bremsstrahlung beam and with electron and positron emerging with 250 Mev at an angle of 30°, q/M is less than 9%.

(3) Because q/M is so small, effects of proton structure are negligible.

(4) It appears to be feasible experimentally.[4]

A coincidence experiment with these parameters, carried out with 10% accuracy, is estimated to probe quantum electrodynamics to 0.3×10^{-13} cm.§

II. DETAILS OF THE PAIR PRODUCTION CALCULATION

The calculations were carried out independently by each of us in order to eliminate algebraic errors.

The form of the pair-production matrix elements in momentum space is[7]

$$\mathfrak{M}_{1a}=\bar{u}(Q')\left\{\gamma_\mu F_1(q^2)-\frac{\mu}{4M}[\gamma_\mu,\boldsymbol{q}]F_2(q^2)\right\}\times u(Q)\bar{u}(p_-)\gamma^\mu\frac{1}{\boldsymbol{k}-\boldsymbol{p}_+-m}\boldsymbol{e}v(p_+),$$

$$\mathfrak{M}_{1b}=\bar{u}(Q')\left\{\gamma_\mu F_1(q^2)-\frac{\mu}{4M}[\gamma_\mu,\boldsymbol{q}]F_2(q^2)\right\}\times u(Q)\bar{u}(p_-)\boldsymbol{e}\frac{1}{\boldsymbol{p}_--\boldsymbol{k}-m}\gamma^\mu v(p_+),$$

$$\mathfrak{M}_{2a}=\bar{u}(Q')\left\{\gamma_\mu+\frac{\mu}{4M}[\gamma_\mu,\boldsymbol{p}_++\boldsymbol{p}_-]\right\}\frac{1}{Q+k-M}\times\left\{\boldsymbol{e}-\frac{\mu}{2M}\boldsymbol{e}\boldsymbol{k}\right\}u(Q)\bar{u}(p_-)\gamma^\mu v(p_+),\tag{1}$$

$$\mathfrak{M}_{2b}=\bar{u}(Q')\left\{\boldsymbol{e}-\frac{\mu}{2M}\boldsymbol{e}\boldsymbol{k}\right\}\frac{1}{Q'-\boldsymbol{k}-M}\times\left\{\gamma_\mu+\frac{\mu}{4M}[\gamma_\mu,\boldsymbol{p}_++\boldsymbol{p}_-]\right\}u(Q)\bar{u}(p_-)\gamma^\mu v(p_+).$$

Table I defines all symbols used in this paper.

By the customary covariant techniques, the matrix elements were squared, summed, and averaged over initial and final polarizations to yield the differential cross section

$$d\sigma=\frac{\alpha^3M}{4\pi^2k}\delta^{(4)}(k-p_+-p_--q)\times\frac{d^3Q'}{E'}\frac{d^3p_+}{E_+}\frac{d^3p_-}{E_-}(\lambda_{11}+\lambda_{12}+\lambda_{22}).\tag{2}$$

λ_{11} represents the contribution from the squares of the

§ *Note added in proof.*—Dr. Richter has informed us that a recalculation of counting rates in the coincidence experiment indicates that an angle in the range 20° to 25° for the electron-positron pair is more reasonable than the value of $\theta=30°$ used in the above discussion and in Secs. IV and V. Such an arrangement probes quantum electrodynamics to $\approx 0.5\times 10^{-13}$ cm. By operating at an incident energy ≈ 1000 Mev and at $\theta=15°$ it appears to be possible to probe down to the nucleon compton wavelength.

[7] We use the notation of Schweber, Bethe, and de Hoffmann, *Mesons and Fields* (Row, Peterson and Company, Evanston, 1955), Vol. 1, and choose $\hbar=c=1$.

diagrams in Fig. 1, λ_{12} that from the interference of those in Fig. 1 with those in Fig. 2, and λ_{22} that from the squares of those in Fig. 2; they have the following forms:

$$\lambda_{11}=\frac{1}{2q^4}\mathfrak{F}_1(q^2)\left\{\frac{m^2q^2}{(k\cdot p_-)^2}-2\left[\frac{k\cdot p_+}{k\cdot p_-}+\frac{k\cdot p_-}{k\cdot p_+}+\frac{q^2p_+\cdot p_-}{k\cdot p_+k\cdot p_-}\right]\right\}$$
$$+\frac{1}{2q^4}\mathfrak{F}_2(q^2)\left\{\frac{2m^2(p_+\cdot P)^2}{(k\cdot p_-)^2}\right.$$
$$\left.-\frac{q^2[(p_+\cdot P)^2+(p_-\cdot P)^2]}{k\cdot p_+k\cdot p_-}\right\}, \quad (3)$$

where

$$\mathfrak{F}_1=\frac{q^2}{M^2}(F_1+\mu F_2)^2+\frac{P^2}{2M^2}\left(F_1^2-\frac{\mu^2q^2}{4M^2}F_2^2\right),$$
$$\mathfrak{F}_2=\frac{1}{M^2}\left(F_1^2-\frac{\mu^2q^2}{4M^2}F_2^2\right); \quad (4)$$

$$\lambda_{12}=\frac{2}{q^2(p_++p_-)^2}\left[2\left(\frac{Q\cdot kp_+\cdot p_-+Q\cdot p_-k\cdot p_+-Q\cdot p_+k\cdot p_-}{k\cdot p_+}\right)\right.$$
$$-2\left(\frac{Q\cdot kp_+\cdot p_-+Q\cdot p_+k\cdot p_--Q\cdot p_-k\cdot p_+}{k\cdot p_-}\right)$$
$$+2(Q\cdot p_+Q'\cdot p_-+Q\cdot p_-Q'\cdot p_+-Q\cdot Q'p_+\cdot p_-)$$
$$\times\left\{\frac{1}{k\cdot Q}\left(\frac{Q\cdot p_-}{k\cdot p_-}-\frac{Q\cdot p_+}{k\cdot p_+}\right)-\frac{1}{k\cdot Q'}\left(\frac{Q'\cdot p_-}{k\cdot p_-}-\frac{Q'\cdot p_+}{k\cdot p_+}\right)\right\}$$
$$+M^2\left(\frac{1}{k\cdot p_+}-\frac{1}{k\cdot p_-}\right)$$
$$\times\left(\frac{k\cdot p_+Q\cdot p_-+k\cdot p_-Q\cdot p_+-k\cdot Qp_+\cdot p_-}{k\cdot Q'}\right.$$
$$\left.\left.-\frac{k\cdot p_+Q'\cdot p_-+k\cdot p_-Q'\cdot p_+-k\cdot Q'p_+\cdot p_-}{k\cdot Q}\right)\right]; \quad (5)$$

$$\lambda_{22}=\frac{1}{(p_++p_-)^4}\left[\frac{4(k\cdot p_+p_-\cdot Q+k\cdot p_-p_+\cdot Q)^2}{(k\cdot Q)^4}\right.$$
$$+\frac{M^2(k\cdot q)^2(p_++p_-)^2}{(k\cdot Q)^4}+\frac{q^2(p_++p_-)^2}{(k\cdot Q)^2}$$
$$\left.-\frac{4(p_++p_-)^2p_+\cdot Qp_-\cdot Q}{(k\cdot Q)^2M^2}+\frac{2(p_++p_-)^2+4m^2}{M^2}\right]. \quad (6)$$

The electron mass was neglected everywhere except in denominators and in terms such as $m^2/(k\cdot p_-)^2$, which give a contribution independent of m when integrated over angles. λ_{11} contains no approximations other than this. In the interference terms λ_{12}, only terms of order q/M and q^2/M^2 relative to the leading order of λ_{11} were kept, which implies that the form factors F_1 and F_2 can be set equal to unity. In λ_{22} only terms of order q^2/M^2 relative to the leading order were retained. It turns out that to these orders there are no contributions to λ_{12} and λ_{22} from the anomalous moment term in the proton current. The result agrees with an earlier calculation of first-order recoil corrections to bremsstrahlung.[8]

The electron angles were integrated over, the integration being made easy by carrying it out in the Lorentz frame in which the electron and recoil proton come off back to back. The method is illustrated in Appendix I. The form factors were expanded in a power series in order to do the integrals,

$$\mathfrak{F}_1\approx(2+a_1q^2/M^2+b_1q^4/M^4),$$
$$\mathfrak{F}_2\approx\frac{1}{M^2}(1+a_2q^2/M^2+b_2q^4/M^4). \quad (7)$$

The integrated laboratory cross section may be written as

$$\frac{d\sigma}{d\Omega_+dE_+}=\frac{\alpha^3}{8\pi M^3}\frac{p_+\cdot Q}{k\cdot Q}(X_{11}+X_{12}+X_{22}), \quad (8)$$

where the X's are dimensionless quantities which we write in units such that $M=1$. In X_{11} terms of order higher than q^3/M^3 have been neglected. In the expressions for X_{12} and X_{22} we have specialized to the case of positrons emitted at an angle of 90° relative to the incident photon momentum. Terms in X_{22} which do not contain the factor $\ln(2E_+E_-/km)$ were found to be

TABLE I. Glossary of symbols.[a]

k	4-momentum of incident γ ray
p_-	4-momentum of outgoing electron
p_+	4-momentum of outgoing positron
Q	4-momentum of initial proton
Q'	4-momentum of recoil proton
e	polarization 4-vector of incident γ ray
m	mass of electron
M	mass of proton
a_μ	proton matrix element $=\bar{u}(Q')\gamma_\mu u(Q)$
θ	angle between p_+ and k in laboratory
Λ	large "regulator" mass in radiative corrections
λ	photon mass (for handling infrared divergences)
α	$1/137$
q	$Q'-Q=k-p_+-p_-$
P	$Q+Q'$
ω	$Q+k-p_+$
ω_0	$(\omega^2)^{\frac{1}{2}}$
E_-	$p_-\cdot\omega/\omega_0$
E_+	$p_+\cdot\omega/\omega_0$
k_0	$k\cdot\omega/\omega_0$
$\mathbf{k}\cdot\mathbf{Q}$	$k\cdot\omega Q\cdot\omega/\omega^2-k\cdot Q$
$\lvert\mathbf{Q}\rvert^2$	$(Q\cdot\omega)^2/\omega^2-1$
A	$2(\omega^2-1)(k-p_+)\cdot Q+4(p_+\cdot Q)^2$
B	$\omega^2-1-2p_+\cdot Q$

[a] Unless otherwise indicated, $P_1\cdot P_2$ indicates the invariant scalar product of 4-vectors; i.e., $P_1\cdot P_2=E_1E_2-\mathbf{P}_1\cdot\mathbf{P}_2$.

[8] S. D. Drell, Phys. Rev. **87**, 753 (1952).

negligible; we do not include them in the following expressions:

$$X_{11}=\frac{8\omega_0E_-}{(k\cdot p_+)^2}-\frac{2\omega_0E_-}{k\cdot\omega k\cdot p_+Q\cdot p_+}[2-4Q\cdot p_++8a_2(Q\cdot p_+)^2]$$
$$+\frac{4E_-\omega_0}{(k\cdot\omega)^2}[a_1-4a_2Q\cdot p_++8b_2(Q\cdot p_+)^2]-\frac{4k\cdot\omega}{k\cdot p_+(Q\cdot p_+)^2}$$
$$\times\left[\ln\frac{2E_-Q\cdot p_+}{mk_0}+\frac{\omega_0E_-(Q\cdot\omega Q\cdot p_+-\omega\cdot p_+)}{k\cdot p_+k\cdot\omega}\right]$$
$$+\frac{2}{Q\cdot p_+(k\cdot p_+)^2}[A+4k\cdot p_++2a_1(k\cdot p_+)^2]\ln\frac{2E_-Q\cdot p_+}{mk_0}$$
$$-\frac{4}{k\cdot\omega k\cdot p_+}[2+B+a_2A+2a_1k\cdot p_+$$
$$+(2b_1+a_2)(k\cdot p_+)^2]\ln\frac{2E_-}{m}+\frac{8}{(k\cdot\omega)^2k\cdot p_+}$$
$$\times[a_1+a_2B+b_2A+(2b_1+a_2)k\cdot p_+]$$
$$\times\left[k\cdot p_+Q\cdot p_+\ln\frac{2E_-}{m}-\mathbf{k}\cdot\mathbf{Q}\omega_0E_-\right]$$
$$-\frac{16(Q\cdot p_+)^2k\cdot p_+}{(k\cdot\omega)^3}[b_1+\tfrac{1}{2}a_2+b_2B]\ln\frac{2E_-}{m}$$
$$-\frac{4\omega_0E_-}{(k\cdot p_+)^3}\left\{k_0E_-+\frac{\mathbf{k}\cdot\mathbf{Q}}{|\mathbf{Q}^2|}[k\cdot p_++(k_0-E_+)E_-]\right\}$$
$$+\frac{4a_1E_-}{\omega_0k\cdot p_+}\left(Q\cdot p_+-2-\frac{\mathbf{k}\cdot\mathbf{Q}}{|\mathbf{Q}^2|}\right)$$
$$+\frac{2}{k\cdot p_+\omega_0|\mathbf{Q}|}\left\{2(1-Q\cdot p_+)+a_1k_0E_-+\frac{\mathbf{k}\cdot\mathbf{Q}}{|\mathbf{Q}^2|}\right.$$
$$\left.\times[1+a_1k\cdot p_++a_1(k_0-E_+)E_-]\right\}$$
$$\times\ln\frac{k\cdot p_++(k_0-E_+)E_-+|\mathbf{Q}|E_-}{k\cdot p_++(k_0-E_+)E_--|\mathbf{Q}|E_-},\quad(9)$$

$$X_{12}=\frac{4}{\omega_0}\left\{\frac{-1}{k_0^3E_+}(7E_+^2+5E_+E_-+2E_-^2)\ln\frac{k_0}{E_+}\right.$$
$$+\frac{1}{k_0^3E_+}(E_+^2-E_+E_-+2E_-^2)\ln2$$
$$\left.+\frac{E_-}{k_0^4E_+^2}(7E_+^3+6E_+^2E_--3E_-^3)\right\},\quad(10)$$

$$X_{22}=\frac{4(E_+^2+E_-^2)}{k_0^2E_+}\ln\frac{2E_+E_-}{k_0m}.\quad(11)$$

$X_{12}/X_{11}=-1\%$ and $X_{22}/X_{11}=+\frac{1}{2}\%$ for $E_+=E_-=70$ Mev. These ratios are slowly varying functions of E_+. If one allows $M\to\infty$, one obtains the result found by Hough,[9] who integrated the Bethe-Heitler formula over angles.

III. RADIATIVE CORRECTIONS

In this section we calculate radiative corrections to σ_{BH} due to virtual and real photons. Since radiative corrections are $<5\%$ in all cases of interest, in evaluating them we have consistently ignored proton recoil and terms of order less than $\alpha\ln(E/m)$ relative to σ_{BH}. For example, radiative corrections to "Compton" diagrams (Fig. 2), and to the proton current in "Bethe-Heitler" diagrams (Fig. 1), involve proton recoil and have been neglected. This leaves radiative corrections to the electron current in "Bethe-Heitler" diagrams to be evaluated.

The virtual radiative matrix elements, Fig. 3, were evaluated under the conditions of the 140-Mev experiment, $|q^2|\sim2k\cdot p_+\gg2k\cdot p_-\gtrsim m^2$. We list these matrix elements individually in a form which allows them to be adapted to other processes.[10] Terms of order less than $\alpha\ln(E/m)$ are neglected. In case $|q^2|\sim2k\cdot p_+\sim2k\cdot p_-\gg m^2$, O_2 and O_{12} differ from the list below and can be obtained from O_1 and O_{11} by the substitution $k\leftrightarrow(-k)$, $p_-\leftrightarrow(-p_+)$, $e\leftrightarrow a$. This substitution is appropriate for the coincidence pair experiment.

$$\mathfrak{M}_1=-\frac{i\alpha}{4\pi^3}\bar{u}(p_-)\int d^4l\left(\frac{1}{l^2-\lambda^2+i\epsilon}-\frac{1}{l^2-\Lambda^2+i\epsilon}\right)$$
$$\times\gamma_\mu\frac{1}{\not p_--\not l-m}\not a\frac{1}{\not k-\not p_+-\not l-m}\gamma^\mu\frac{1}{\not k-\not p_+-m}ev(p_+)$$
$$\equiv\bar{u}(p_-)O_1v(p_+),\quad(12)$$

$$O_1=\frac{\alpha}{4\pi}\left[\ln\frac{\Lambda^2}{m^2}+\left(1+\frac{q^2}{p_-\cdot q}\ln\frac{-q^2}{2k\cdot p_+}\right)\ln\frac{-q^2}{m^2}\right]\not a\frac{1}{\not k-\not p_+-m}e$$
$$-\frac{\alpha}{4\pi p_-\cdot q}\left[1+\frac{q^2}{2p_-\cdot q}\ln\frac{-q^2}{2k\cdot p_+}\right]\ln\frac{-q^2}{m^2}ap_-e,$$

$$O_2=\frac{\alpha}{4\pi}\left\{\ln\frac{\Lambda^2}{m^2}+\left(1+\frac{6k\cdot p_-}{q^2}\right)\ln\frac{-q^2}{m^2}\right.$$
$$+2\left(1+\frac{3k\cdot p_-}{q^2}\right)\ln\frac{-q^2}{2k\cdot p_-}-\left[1-8\left(\frac{k\cdot p_-}{q^2}\right)^2\right]$$
$$\left.\times\ln\frac{-q^2}{2k\cdot p_-}\ln\frac{-q^6}{2m^4k\cdot p_-}\right\}e\frac{1}{\not p_--\not k-m}a$$
$$+\frac{\alpha}{4\pi}\left[-2\ln\frac{-q^2}{m^2}-3\ln\frac{-q^2}{2k\cdot p_-}\right.$$
$$\left.+\left(1-\frac{2k\cdot p_-}{q^2}\right)\ln\frac{-q^2}{2k\cdot p_-}\ln\frac{-q^6}{2m^4k\cdot p_-}\right]\frac{ep_+a}{q^2},$$

[9] P. V. C. Hough, Phys. Rev. **74**, 80 (1948).

[10] This differs from the radiative correction to Compton scattering [L. M. Brown and R. P. Feynman, Phys. Rev. **85**, 231 (1952)] where both vertices correspond to $k^2=q^2=0$. The calculation of radiative corrections to bremsstrahlung by A. N. Mitra [Nature **169**, 1009 (1952)] applies only to low-momentum transfers.

$$O_3=\frac{\alpha}{4\pi}\left[\ln\frac{\Lambda^2}{2k\cdot p_+}\frac{\not a}{\not k-\not p_+-m}\not e-\ln\frac{2k\cdot p_+}{m^2}\frac{\not a\not k\not e}{k\cdot p_+}\right],$$

$$O_4=\frac{\alpha}{4\pi}\left[\ln\frac{\Lambda^2}{2k\cdot p_-}\frac{\not e}{\not p_--\not k-m}\not a+\ln\frac{2k\cdot p_-}{m^2}\frac{\not e\not k\not a}{k\cdot p_-}\right],$$

$$O_5=O_6=-\frac{\alpha}{4\pi}\left(\tfrac{1}{2}\ln\frac{\Lambda^2}{m^2}-\ln\frac{m^2}{\lambda^2}\right)\not a\frac{1}{\not k-\not p_+-m}\not e,$$

$$O_7=O_8=-\frac{\alpha}{4\pi}\left(\tfrac{1}{2}\ln\frac{\Lambda^2}{m^2}-\ln\frac{m^2}{\lambda^2}\right)\not e\frac{1}{\not p_--\not k-m}\not a,$$

$$O_9=-\frac{\alpha}{4\pi}\ln\frac{\Lambda^2}{2k\cdot p_+}\frac{\not a}{\not k-\not p_+-m}\not e, \tag{13}$$

$$O_{10}=-\frac{\alpha}{4\pi}\ln\frac{\Lambda^2}{2k\cdot p_-}\frac{\not e}{\not p_--\not k-m}\not a,$$

$$O_{11}=\frac{\alpha}{2\pi}\ln\frac{2p_-\cdot p_+}{m^2}\left[\left(-\ln\frac{m^2}{\lambda^2}-\tfrac{1}{2}\ln\frac{2p_+\cdot p_-}{m^2}-\frac{q^2}{2p_-\cdot q}\ln\frac{-q^2}{2p_+\cdot k}\right)\not a\frac{1}{\not k-\not p_+-m}\not e+\frac{\not a\not p_+\not e}{2k\cdot p_+}+\left(1+\frac{q^2}{2p_-\cdot q}\ln\frac{-q^2}{2p_+\cdot k}\right)\frac{\not a\not p_-\not e}{2p_-\cdot q}\right],$$

$$O_{12}=-\frac{\alpha}{4\pi}\ln\frac{q\cdot p_+}{p_-\cdot p_+}\ln\frac{-q^2}{2p_-\cdot k}\frac{\not p_+\not e\not a}{k\cdot p_+}+\frac{\alpha}{2\pi}\left\{\tfrac{1}{2}\left(\ln\frac{-q^2}{2k\cdot p_-}\right)^2+\ln\frac{2p_+\cdot p_-}{m^2}\times\left[-\ln\frac{m^2}{\lambda^2}-\tfrac{1}{2}\ln\frac{2p_+\cdot p_-}{m^2}-\frac{q^2}{2p_+\cdot q}\ln\frac{-q^2}{2k\cdot p_-}\right]\right\}\times\not e\frac{1}{\not p_--\not k-m}\not a+\frac{\alpha}{2\pi}\ln\frac{2p_-\cdot p_+}{m^2}\times\left[\frac{-\not e\not p_-\not a}{2k\cdot p_-}-\left(1+\frac{q^2}{2p_+\cdot q}\ln\frac{-q^2}{2k\cdot p_-}\right)\frac{\not e\not p_+\not a}{2p_+\cdot q}\right],$$

$$O_{13}=\frac{\alpha}{3\pi}\ln\left(\frac{-q^2}{m^2}\right)\not a\frac{1}{\not k-\not p_+-m}\not e,$$

$$O_{14}=\frac{\alpha}{3\pi}\ln\frac{-q^2}{m^2}\not e\frac{1}{\not p_--\not k-m}\not a,$$

Adding together $O_1\cdots O_{14}$ we obtain

$$O_{\text{total}}=\frac{\alpha}{2\pi}\left\{\ln\frac{2p_-\cdot p_+}{m^2}\left[-\ln\frac{m^2}{\lambda^2}-\tfrac{1}{2}\ln\frac{2p_+\cdot p_-}{m^2}+\frac{13}{6}\right]+\ln\frac{m^2}{\lambda^2}-\ln\frac{-q^2}{2p_-\cdot p_+}\ln\frac{-q^2}{2k\cdot p_-}\right\}\times\left(\not a\frac{1}{\not k-\not p_+-m}\not e+\not e\frac{1}{\not p_--\not k-m}\not a\right), \tag{14}$$

where we have anticipated the angular integrals leading to the total cross section and neglected all terms which do not survive in the integrated σ to order $\alpha\ln(E/m)$.

The lowest order radiative correction to the cross section due to virtual photons is provided by the interference of O_{total} with $\mathfrak{M}_{1a}$ and $\mathfrak{M}_{1b}$ in Eq. (1) and is conveniently divided into two parts:

$$\sigma(\text{virtual})=\sigma(\text{virtual infrared})+\sigma(\text{virtual remainder}). \tag{15}$$

σ(virtual infrared) will cancel with the infrared contributions from real photon emission:

$$\sigma(\text{virtual infrared})=-\frac{\alpha}{\pi}\int d\Omega_-\sigma_{BH}(\Omega_-)\times\left[\ln\frac{2p_-\cdot p_+}{m^2}\left(\ln\frac{m^2}{\lambda^2}+\tfrac{1}{2}\ln\frac{2p_+\cdot p_-}{m^2}\right)-\ln\frac{m^2}{\lambda^2}\right]. \tag{16}$$

Upon integration over electron angles for the experimental condition of interest, i.e., $\mathbf{k}\cdot\mathbf{p}_+=0$, one obtains[11] for σ(virtual remainder)

$$\sigma(\text{virtual remainder})=\frac{\alpha}{2\pi}\sigma_{BH}\ln\frac{2E_+E_-}{m^2}\left[\frac{13}{3}-\ln\frac{E_+}{E_-}\right]. \tag{17}$$

Radiative corrections of the same order occur due to emission of real photons of energy less than ΔE, the energy resolution of the experiment. The cross section corresponding to the Feynman graphs in Fig. 4 has been calculated through order $\alpha\ln(E/m)$, again with neglect of proton recoil corrections, and with $\mathbf{k}\cdot\mathbf{p}_+=0$. We write

$$\sigma(\text{real})=\sigma(\text{real infrared})+\sigma(\text{real remainder}), \tag{18}$$

where σ(real infrared) is obtained by integrating the infrared matrix element,

$$\mathfrak{M}^\mu(\text{infrared})=\frac{e}{[2l_0(2\pi)^3]^{\frac{1}{2}}}\left(\frac{p_-^\mu}{p_-\cdot l}-\frac{p_+^\mu}{p_+\cdot l}\right)\mathfrak{M}_{BH}, \tag{19}$$

[11] Although $\mathbf{k}\cdot\mathbf{p}_+=0$ in the laboratory and the integration is done in the special Lorentz frame of Appendix I, the laboratory and integration frames differ only by proton recoil which has been consistently neglected in radiative corrections.

using a minimum photon mass λ as in the above treatment of virtual corrections. There results

σ(real infrared)

$$=-\frac{\alpha}{\pi}\int d\Omega_- \sigma_{BH}(\Omega_-)\left[\ln\frac{2p_-\cdot p_+}{m^2}\times\left(\ln\frac{m^2}{\lambda^2}+\tfrac{1}{2}\ln\frac{2p_-\cdot p_+}{m^2}-\ln\frac{E_+E_-}{(\Delta E)^2}\right)-\ln\frac{m^2}{\lambda^2}\right], \quad (20)$$

σ(real remainder)

$$=\frac{-\alpha^4 dE_+ d\Omega_+}{4\pi^2}\left(\ln\frac{2E_-}{m}\right)^2\left[\frac{1}{6k_0E_+^2}+\frac{4}{3k_0^3}+\frac{9E_-^2}{k_0^3E_+^2}+\frac{8E_-}{3k_0^4}+\left(\frac{4}{k_0^3}-\frac{10}{k_0^2E_+}+\frac{5}{k_0E_+^2}\right)\ln\frac{k_0}{E_+}\right]. \quad (21)$$

The λ-dependent terms cancel when real and virtual contributions are added, leaving a finite total[12] radiative correction

$$\sigma(\text{radiative})=\frac{-\alpha}{\pi}\sigma_{BH}\ln\frac{2E_-E_+}{m^2}\times\left(\ln\frac{E_+E_-}{(\Delta E)^2}-\frac{13}{6}+\tfrac{1}{2}\ln\frac{E_+}{E_-}\right)+\sigma(\text{real remainder}), \quad (22)$$

with σ_{BH} given by Eq. (8) and σ(real remainder) given by Eq. (21). In the 140-Mev experiment one finds $\Delta E=E_-$, the energy of the unobserved electron. This is then a low-resolution experiment, with resolution logarithm of the order of unity, and all terms in Eq. (22) are comparable in magnitude. For this experiment the radiative corrections are numerically[13] less than 1%, with errors estimated at 1%.

IV. COINCIDENCE EXPERIMENT CALCULATION

The electron and positron are observed at equal angles [$\theta=\angle(\mathbf{k},\mathbf{p}_+)=\angle(\mathbf{k},\mathbf{p}_-)$] and energies in the coincidence experiment, because interference terms vanish identically under these conditions as is discussed below. The additional condition that $\mathbf{p}_+$, $\mathbf{k}$, and $\mathbf{p}_-$ are in the same plane is imposed to minimize proton recoil and the importance of the Compton trace λ_{22} relative to the Bethe-Heitler trace λ_{11}.

In the coincidence experiment m^2 terms can be ignored, since all denominators are far off the energy shell. Also $k\cdot p_-=k\cdot p_+$, $Q\cdot p_-=Q\cdot p_+$, and $Q'\cdot p_-=Q'\cdot p_+$. Equation (3) for λ_{11} then simplifies to

$$\lambda_{11}=\frac{-1}{q^4}\mathfrak{F}_1(q^2)\left[2+\frac{q^2p_+\cdot p_-}{(k\cdot p_+)^2}\right]-\frac{1}{q^2}\mathfrak{F}_2(q^2)\frac{(p_+\cdot P)^2}{(k\cdot p_+)^2}. \quad (23)$$

All quantities appearing in the coincidence experiment are to be evaluated in the laboratory. The laboratory cross section for incident photon spectrum $G(k)$ is

$$\sigma_{BH}=\frac{\alpha^3M}{4\pi^2}\frac{d^3p_+}{E_+}\frac{d^3p_-}{E_-}\times\int\frac{d^3Q'}{E'}\frac{dk}{k}G(k)\delta^{(4)}(k-p_+-p_--q)\lambda_{11}=\frac{\alpha^3M}{4\pi^2}\frac{d^3p_+}{E_+}\frac{d^3p_-}{E_-}\frac{G(\kappa)}{2p_+\cdot Q-p_+\cdot p_-}\lambda_{11}(\kappa), \quad (24)$$

where

$$\kappa=\frac{2p_+\cdot Q-p_+\cdot p_-}{M-2E_++2E_+\cos\theta}. \quad (25)$$

The form factors are so close to unity for these conditions that experimental uncertainty in the proton size has negligible effect on the cross section. σ_{BH} contains no approximations except for neglect of m^2 terms, which are order m^2/E^2.

On account of the existence of a mirror plane of symmetry between p_+ and p_-, one has $\sigma(p_+,p_-)=\sigma(p_-,p_+)$. On the other hand, the electron trace representing interference between one-photon (Compton) and two-photon (Bethe-Heitler) electron matrix elements behaves like three photons under charge conjugation, and is antisymmetric under interchange of p_- and p_+. As a result, λ_{12} vanishes identically, independent of meson effects. The antisymmetry of λ_{12} in p_+ and p_- ensures that the interference cross section vanishes even when integrated over the experimental angle and energy spread, provided that the experimental conditions are symmetric in p_+ and p_-.

λ_{22} is unknown above the meson resonance. Under the conditions of this experiment the quantum electrodynamics value of λ_{22}, with neglect of proton recoil, is

$$\lambda_{22}=(E_+^2/M^2)\tan^4(\theta/2)\lambda_{11}. \quad (26)$$

Even when multiplied by ten as an estimate of the effect of the meson resonance, λ_{22} amounts to only $\frac{1}{2}$% for $E_+=250$ Mev and $\theta=30°$. Thus λ_{22} may be neglected, provided E_+ and θ are not too large.

[12] Other terms of order $\alpha[\ln(E/m)]^2$ appeared in both virtual (viz., O_2 and O_{12}) and real radiative cross sections, but cancelled out of the total σ(virtual) and independently out of the total σ(real). An heuristic but regrettably lengthy and unphysical argument can be made [see S. C. Frautschi, Ph.D. thesis, Stanford University (unpublished)] which suggests that aside from the ΔE-dependent term, terms of order $\alpha[\ln(E/m)]^2$ always cancel out of lowest order quantum electrodynamics radiative corrections. Some other cases where this has been verified are J. Schwinger, Phys. Rev. **75**, 897 (1949); S. N. Gupta, Phys. Rev. **98**, 1502 (1955); R. G. Newton, Phys. Rev. **98**, 1514 (1955); M. Chrétien, Phys. Rev. **98**, 1515 (1955).

[13] In the region of experimental interest, individual terms of σ(radiative) are $\lesssim 5\%$, and there are strong cancellations. The cancellations persist outside the experimental region, and the total σ(radiative) is still $\sim 1\%$ for $E_+\ll K$.

For a given bremsstrahlung spectrum, the experimental parameters for the coincidence experiment will be determined by a compromise between

(1) the desire to maximize $2k\cdot p_+=4kE_+\sin^2(\theta/2)$, the extent to which the electron propagator leaves the energy shell and small distances are probed, a desire which suggests large E_+ and θ;

(2) the necessity that σ_{BH} be observable and greater than the chance coincidence rate, and that $\lambda_{22}/\lambda_{11}$ be small, which together require E_+ and θ to be small.

Virtual radiative matrix elements are evaluated under the conditions $|q^2|\sim k\cdot p_+=k\cdot p_-\gg m^2$, with neglect of proton recoil and terms of order less than $\alpha\ln(E/m)$. Under these conditions the matrix elements of Eq. (13) are still valid except for O_2 and O_{12} which must be obtained from O_1 and O_{11}, respectively, by the substitutions $k\leftrightarrow(-k)$, $p_-\leftrightarrow(-p_+)$, $e\leftrightarrow a$. Then the total virtual radiative matrix element is given by Eq. (14) with the last term omitted. The resulting lowest order radiative correction to the coincidence cross section due to virtual photons is

$$\sigma(\text{virtual})=-\frac{\alpha}{\pi}\sigma_{BH}\left[\ln\frac{2p_+\cdot p_-}{m^2}\times\left(\ln\frac{m^2}{\lambda^2}+\tfrac{1}{2}\ln\frac{2p_+\cdot p_-}{m^2}-\frac{13}{6}\right)-\ln\frac{m^2}{\lambda^2}\right]. \quad (27)$$

The effective energy resolution ΔE is determined by how far the incident bremsstrahlung spectrum extends above κ. Under experimental conditions, ΔE will be sufficiently small that the infrared matrix element, Eq. (19), can be taken to represent the contribution of real radiative photons. Then, with neglect of proton recoil and terms of order $\alpha(\Delta E/E)\ln(E/m)$ or less, real photon emission is given by

$$\sigma(\text{real})=\frac{\alpha}{\pi}\sigma_{BH}\left[\ln\frac{2p_-\cdot p_+}{m^2}\times\left(\ln\frac{m^2}{\lambda^2}+\tfrac{1}{2}\ln\frac{2p_+\cdot p_-}{m^2}-\ln\frac{E_+E_-}{(\Delta E)^2}\right)-\ln\frac{m^2}{\lambda^2}\right]. \quad (28)$$

As a result, the total radiative cross section has the same form as the Schwinger correction to electron-proton scattering,[14]

$$\sigma(\text{radiative})=-\frac{2\alpha}{\pi}\ln\frac{2p_+\cdot p_-}{m^2}\left[\ln\frac{E_+}{\Delta E}-\frac{13}{12}\right]\sigma_{BH}, \quad (29)$$

with ΔE defined by

$$\int_\epsilon^\infty\frac{G(\kappa+l)dl}{l}\equiv G(\kappa)\ln\frac{\Delta E}{\epsilon}, \quad (30)$$

and σ_{BH} by Eq. (24).

[14] J. Schwinger, Phys. Rev. **75**, 897 (1949).

For $E_+=250$ Mev, and $\theta=30°$, σ(radiative) has the value $-0.03\sigma_{BH}$ when $\Delta E=50$ Mev, and $-0.083\sigma_{BH}$ when $\Delta E=20$ Mev. The errors in σ(radiative) are

(1) errors of order α in σ(virtual),

(2) errors of order $\alpha(\Delta E/E)\ln(E/m)$ in σ(real), and

(3) errors of order $\alpha(q/M)\ln(E/m)\ln(E/\Delta E)$ in neglected diagrams.

Together, these are estimated to be $<2\%$ of σ_{BH}.

V. CONCLUSION

Wide-angle pair production has been analyzed as a probe of quantum electrodynamics at small distances. Cross sections for two experimental situations have been evaluated.

(1) The cross section for observation of positrons at right angles to a 140-Mev γ ray is given by Eqs. (8–11) and (22). Estimated errors are $<2\%$ from the experimental proton form factor, $<1\%$ from X_{12}, and $<1\%$ from radiative corrections. The cross section for observation of 85-Mev positrons at right angles is 6.6×10^{-35} cm^2/Mev-sterad. Experimental confirmation of this number within an accuracy of 5% is estimated to test the electron propagator in quantum electrodynamics to $\sim0.7\times10^{-13}$ cm. At present the agreement between theory and experiment is[15]

$$\sigma_{\text{exp}}/\sigma_{\text{th}}=0.96\pm0.14.$$

(2) The cross section for observation of positrons and electrons in coincidence, at equal energies and angles, is the sum of Eqs. (24) and (29). Estimated errors are $<2\%$ for radiative corrections, and $<\frac{1}{2}\%$ for σ_{Compton} [Eq. (26)] at $E_-=E_+=250$ Mev and $\theta=30°$. Equation (24) differs from the Bethe-Heitler cross section by -2% due to form factors, $+6\%$ due to anomalous moment, and -20% due to proton recoil for these parameters. The differential cross section is calculated to be 1.5×10^{-35} cm^2/Mev (sterad)^2, and if measured to an accuracy of 10% will provide a test of quantum electrodynamics to $\sim0.3\times10^{-13}$ cm.

We have carried through these calculations using standard Feynman-Dyson methods. Although we have no alternative to offer, we feel that this has been an inefficient procedure since large cancellations were found between individually non-gauge-invariant contributions, especially in the calculations of radiative corrections and interference terms.[16] In particular no terms of order $\alpha\ln^2(E/m)$ survived.

Agreement between experiment and the calculations presented in this paper will extend our knowledge of the electron propagator to smaller distances than achieved so far.[17] In particular a coincidence arrangement ap-

[15] B. Richter, Bull. Am. Phys. Soc. Ser. II, **3**, 45 (1958). We thank Dr. Richter for discussions of his results prior to publication.

[16] We now feel that the calculation would have been considerably simpler had we, e.g., combined O_2, O_4, and O_{12} over a common denominator before performing the integrations.

[17] The distances achieved so far are estimated to be (2 to 5) $\times10^{-13}$ cm in reference 1. A separate estimate not given there in-

pears capable of testing the electron propagator at distances approaching the nucleon Compton wavelength, which is comparable with our present limit on the photon propagator.[1]

On the other hand, a discrepancy between theory and experiment can be attributed only to a breakdown of the present theory of quantum electrodynamics as applied to the electron.

APPENDIX I. METHOD OF ANGULAR INTEGRATION

Consider a typical angular integral:

$$I=\int \frac{d^3p_-}{E_-}\frac{d^3Q'}{E'}\delta^{(4)}(\omega-p_--Q')\frac{1}{(k\cdot p_-)q^2}.$$

Writing

$$\int \frac{d^3Q'}{E'}=2\int d^4Q'\,\delta(Q'^2-M^2)\eta(Q_0'),$$

and then carrying out the integration of the 4-dimensional δ-function over d^4Q', one obtains (neglecting m^2)

$$I=2\int \frac{d^3p_-}{E_-}\delta(\omega^2-2\omega\cdot p_--M^2)\frac{1}{k\cdot p_-q^2}.$$

I is an invariant and may be evaluated in any coordinate frame. The easiest is that defined by $\omega=(\omega_0,0)$, since for that choice the δ-function contains no angular dependence. In that frame

$$I=\int \frac{E_-}{\omega_0}d\Omega_-\frac{1}{k\cdot p_-q^2}$$
$$=\int_0^1 dz\int d\Omega_-\frac{E_-}{\omega_0}\frac{1}{[k\cdot p_-z+q^2(1-z)]^2}.$$

The rest of the evaluation is straightforward and yields

$$I=\frac{-\pi}{\omega_0 k\cdot p_+(k_0-E_-)}\ln\frac{4E_-^2(k\cdot p_+)(k_0-E_-)^2}{m^2k_0^2[k\cdot p_++2E_-(k_0-E_+-E_-)]}$$
$$=\frac{-2\pi}{k\cdot p_+Q\cdot p_+}\ln\frac{(\omega^2-M^2)Q\cdot p_+}{Mmk\cdot\omega}.$$

volves the effect on the hydrogen atom energy levels due to a modification of the electron propagator at small distances. Since corrections of this type to the energy levels emerge as integrals over hydrogen atom wave functions, they are highly sensitive to the assumed form of the modification. Thus cutoffs of form $\exp[(p_\mu p^\mu-m^2)R^2]$ lead to $\sim$0.1 megacycle/sec correction for $R\sim0.6\times10^{-13}$ cm, while cutoffs of form $\exp[-(p_\mu p^\mu-m^2)^2R^4]$ lead to negligible corrections. Neither of these forms is gauge invariant.